Electrocatalytic activity of ultrathin 2D phosphorene based heteroelectrocatalyst for photoelectrochemical cells

Munkhbayar Batmunkh,[a] Aabhash Shresta,[b,c] Munkhjargal Bat-Erdene,[a] Md. J. Nine,[b] Cameron J. Shearer,[a] Christopher T. Gibson,[a] Ashley D. Slattery,[d] Sherif A. Tawfik,[e] Michael J. Ford,[e] Shizhang Qiao,[b] Sheng Dai,[b,f] and Joseph G. Shapter*[a]

[a] College of Science and Engineering, Flinders University, Bedford Park, Adelaide, South Australia 5042, Australia

[b] School of Chemical Engineering, The University of Adelaide, Adelaide, South Australia 5005, Australia

[c] Nanotechnology Research Laboratory, Research School of Engineering, Australian National University, Canberra, ACT 2601, Australia

[d] Adelaide Microscopy, The University of Adelaide, Adelaide, South Australia 5005, Australia

[e] School of Mathematical and Physical Sciences, University of Technology Sydney Ultimo, New South Wales 2007, Australia

[f] School of Chemical Engineering and Advanced Materials, Newcastle University, Newcastle Upon Tyne NE1 7RU, United Kingdom

Research into efficient synthesis, fundamental properties and potential applications of phosphorene is currently the subject of intense investigation. Herein, solution processed phosphorene or few-layer black phosphorus (FL-BP) sheets are prepared using microwave-exfoliation method and used in photoelectrochemical cells. Based on our experimental and theoretical (density-functional theory (DFT)) studies, we found that the FL-BP sheets can act as catalytically active sites and show excellent electrocatalytic activity for triiodide reduction in dye-sensitized solar cells. Importantly, the device fabricated based on our newly designed cobalt sulfide (CoS_x) decorated nitrogen, sulfur co-doped carbon nanotubes heteroelectrocatalyst coated with FL-BP (FL-BP@N, S-doped CNTs–CoS_x) displayed an impressive photovoltaic efficiency of 8.31%, outperforming expensive platinum counter electrode based cells. This work paves the way for advancing phosphorene research and using phosphorene based electrocatalysts for next-generation energy-storage systems.

Keywords: Black phosphorus, phosphorene, electrocatalyst, solar cells, photochemistry

Since its first discovery by two independent research groups in 2014,[1, 2] phosphorene has attracted interest for a wide range of applications such as transistors,[1, 2] supercapacitors,[3] batteries,[4] photocatalysis,[5] sensors[6] and solar cells[7-9] owing to its unique structure and fascinating properties. These properties include strong anisotropic transport, high ON/OFF ratio, excellent electron and hole mobility, and readily tunable bandgap values.[10-13] Although excellent progress has been made in phosphorene research, there are very few reports available on electrocatalysis by phosphorene.[14-17] What has been reported has focused on using phosphorene and/or few-layer black phosphorus (FL-BP) nanosheets as electrocatalysts for either the hydrogen evolution reaction (HER)[14, 15] or the oxygen evolution reaction (OER)[16, 17]. In addition, producing high quality phosphorene sheets via fast, efficient and simple production methods has been very challenging.

One of important applications of electrocatalysts is dye-sensitized solar cell (DSSC).[18] A typical DSSC is fabricated based on platinum (Pt) electrocatalyst, which serves an essential role in reducing I_3^- to I^- in the system.[19] Due to the high cost and scarcity of the Pt, finding alternative electrocatalysts to the conventional Pt is of great importance. Considerable progress has been made in developing Pt-free electrocatalysts for DSSCs.[20-22] Despite this, the search for novel and efficient alternatives to Pt in DSSCs is still a very active area of research.

Here we demonstrate that FL-BP sheets produced using microwave (MW) assisted liquid-phase exfoliation (LPE) can be used as efficient electrocatalysts to reduce I_3^- to I^- in DSSCs. More importantly, our newly designed heteroelectrocatalyst (cobalt sulfide (CoS_x) decorated nitrogen, sulfur co-doped carbon nanotubes (N, S-doped CNTs–CoS_x)) coated with FL-BP sheets outperformed the expensive Pt, in terms of PV efficiency in DSSCs.

FL-BP sheets were synthesized according to the method discovered recently by our group using a MW-assisted LPE.[23, 24] **Figure 1**a depicts the UV-vis spectrum of our FL-BP solution, showing three main absorption peaks at 240, 300 and 370 nm.[23] Except our FL-BP solution, there has been no experimental work on solution processed FL-BP sheets showing these three strong and sharp peaks. Furthermore, as shown in Figure 1b, our FL-BP sample mainly consists of few-layer (> 4 layers) to multi-layer sheets and has relatively low yields of 1 to 3 layer flakes (see inset).[2, 25]

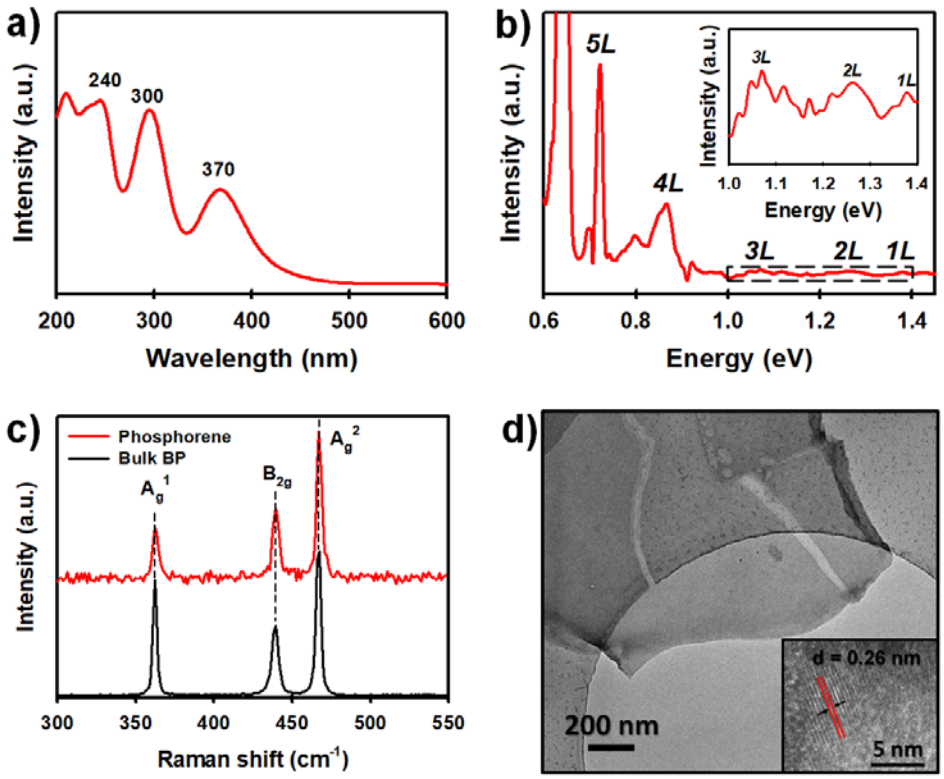

Figure 1. (a) UV-vis, (b) NIR, (c) Raman spectrum and (d) TEM of phosphorene produced using MW-exfoliation.

It can be seen from Figure 1c that there was no shift in the Raman spectrum of the bulk BP after the MW-exfoliation. According to Favron et al.[26], this was expected because the average layer number of our FL-BP sample is more than 4 layers.[23, 24] The transmission electron microscopy (TEM) image of our FL-BP reveals that the flake is very transparent, indicating it is an ultrathin FL-BP sheet (Figure 1d). The lattice spacing of our FL-BP sheet was measured to be 0.26 nm.

To explore the electrocatalytic properties of our FL-BP sheets, we designed a novel carbon based heteroelectrocatalyst, that is N, S-doped CNTs–CoS_x. We note that our N, S-doped CNTs–CoS_x was prepared based on a 1-step synthesis method. The synthesis details can be found in the Experimental Section (Supporting Information). Inspired by recent success of polydopamine (PDA) to produce efficient carbon based electrocatalysts,[27, 28] PDA was used as the N source to generate catalytically active N-doped carbon. The presence of each element (C, N, O, S and Co) in our N, S-doped CNTs–CoS_x was confirmed by a combination of X-ray photoelectron spectroscopy (XPS) (**Figure 2**a) and Energy-dispersive X-ray spectroscopy (EDX) elemental mapping (Figure 2d). The successful heteroatom (S, N) doping of the CNTs was corroborated by the high-resolution XPS (C 1s, N 1s) (see Figure 2b

and Figure S2). Moreover, it can be clearly seen from the TEM image (Figure 2c) that the CoS_x nanoparticles decorated the nanotubes. The CoS_x nanoparticles had high crystallinity; and the lattice constant was measured to be 1.93 Å, corresponding to the (102) planes (see inset of Figure 2c).[29] The successful decoration of the CoS_x nanoparticles on the CNTs was further confirmed by EDX elemental mapping using the scanning TEM (STEM) Figure S3).

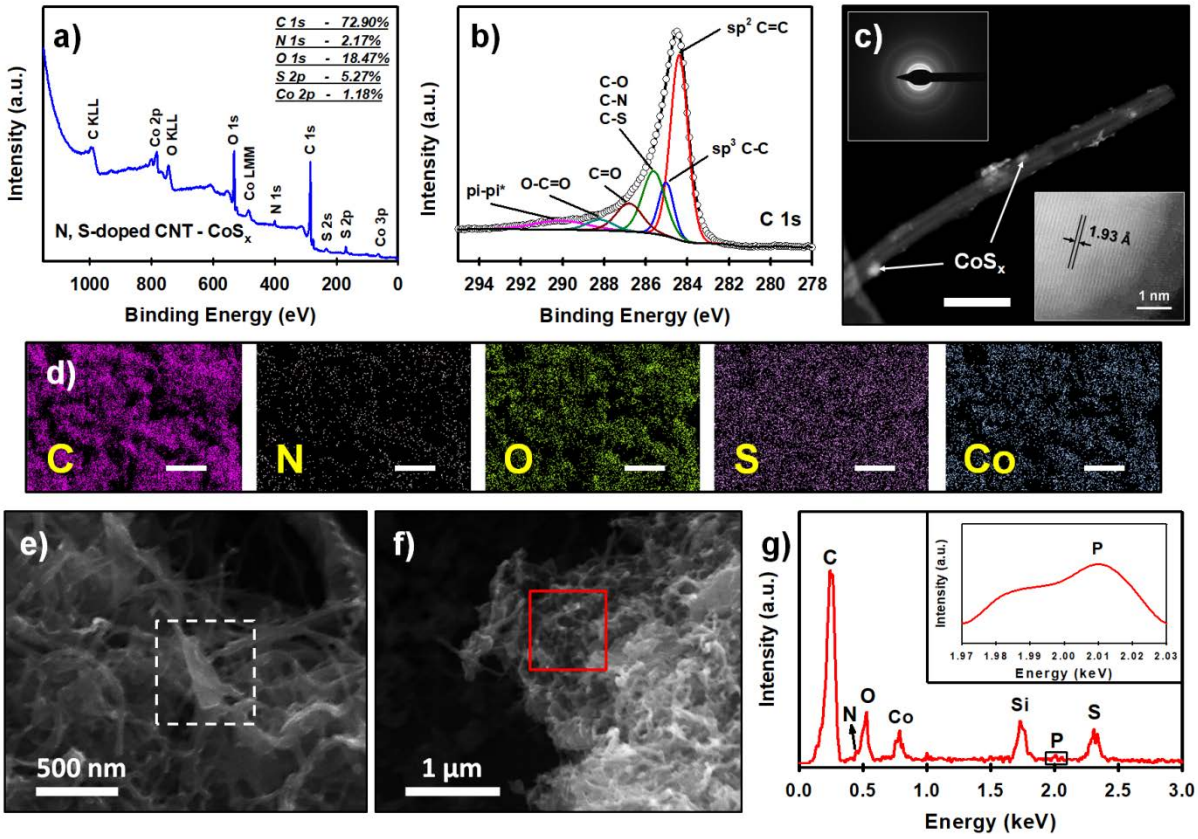

Figure 2. (a) The survey XPS spectrum, (b) high-resolution XPS spectrum of C 1s, (c) TEM image (scale bar: 100 nm) (inset shows the HRTEM and SAED pattern of the CoS_x), and (d) EDX elemental mapping of N, S-doped CNTs–CoS_x (scale bar: 10 µm), demonstrating homogeneous distribution of each elements in the sample. (e and f) SEM images and (g) EDX spectrum of FL-BP@N, S-doped CNTs–CoS_x on the selected area of SEM image shown in (f).

FL-BP@N, S-doped CNTs–CoS_x was prepared by drop-casting FL-BP dispersion onto the N, S-doped CNTs–CoS_x electrode. As shown in Figure 2e, 2D nanosheets with ~500 nm in lateral size were successfully coated onto the nanotubes. EDX spectrum (Figure 2g) on the selected area in Figure 2f further confirms the existence of all elements in the FL-BP@N, S-doped CNTs–CoS_x.

DSSCs were fabricated using the three electrocatalysts, namely the control Pt, N, S-doped CNTs–CoS_x without and coated with FL-BP sheets (**Figure 3**a). Detailed PV parameters of these cells are summarized in Table S1. The control Pt based device exhibited a PCE of up to 7.97%. Our newly designed heteroelectrcatalyst (N, S-doped CNTs–CoS_x) based DSSC showed an efficiency of up to 7.75%, comparable to that of the Pt based cells. Interestingly, after coating FL-BP onto this heteroelectrocatalyst, the PCE of the device increased to 8.31% outperforming cells using Pt.

Increased J_{sc} and *FF* values of the FL-BP@N, S-doped CNTs–CoS_x were the major contributions to this PCE enhancement. A clear improvement in incident-photon-to-current conversion efficiency (IPCE) spectra across the entire wavelength range (from 400 to 700 nm) further confirms the J_{sc} enhancement of the cell after adding FL-BP (Figure 3b). Recently, Yang et al.[9] reported a significant increase in the J_{sc} of DSSCs by adding BP derivatives in the photocathodes and attributed this J_{sc} enhancement to the NIR light absorption of the BP. However, no change in the IPCE spectra in NIR region (800–1100 nm) after adding FL-BP sheets was observed in our study (see inset of Figure 3b). Indeed, we observed slight improvement in the IPCE spectra of the device at wavelengths between 550–700 nm (Figure S4).

We further studied the electrocatalytic activity of our electrocatalysts for triiodide reduction reaction using cyclic voltammetry (CV) and electrochemical impedance spectroscopy (EIS). The peak separation between the anodic and cathodic peaks (E_{pp}) is the main parameter to evaluate the electrocatalytic activity and can be calculated from the CV measurements (Figure 3c). The low E_{pp} indicates high catalytic activity.[27] Surprisingly, the E_{pp} of the N, S-doped CNTs–CoS_x was reduced from 0.196 V to 0.173 V after introducing FL-BP sheets, indicating that the addition of FL-BP improved the electrocatalytic activity. This E_{pp} value was significantly lower than that of the Pt electrocatalyst (0.405 V).

A typical Nyquist plot for Pt electrodes shows two semicircles. The one at lower frequency is associated with the Nernst diffusion impedance (Z_N) corresponding to diffusion of electrolytes, while the other at higher frequency can be related to the charge transfer resistance (R_{ct}) originating from the interface between electrocatalyst and electrolyte.[22, 27] Unlike Pt electrodes, carbonaceous electrodes exhibit an extra semicircle originating from the secondary Nernst diffusion impedance caused by the diffusion through pores (Z_{pore}).[22, 27] From EIS measurements, the FL-BP coated heteroelectrocatalyst exhibited the smallest R_{ct} value (5.47 Ω), which was lower than that of the N, S-doped CNTs–CoS_x (7.87 Ω) and even Pt (6.66 Ω) (Figure 3d). Importantly, our FL-BP@N, S-doped CNTs–CoS_x showed excellent

electrochemical stability in liquid iodide electrolyte with very little change observed over 25 cycles. (Figure S5).

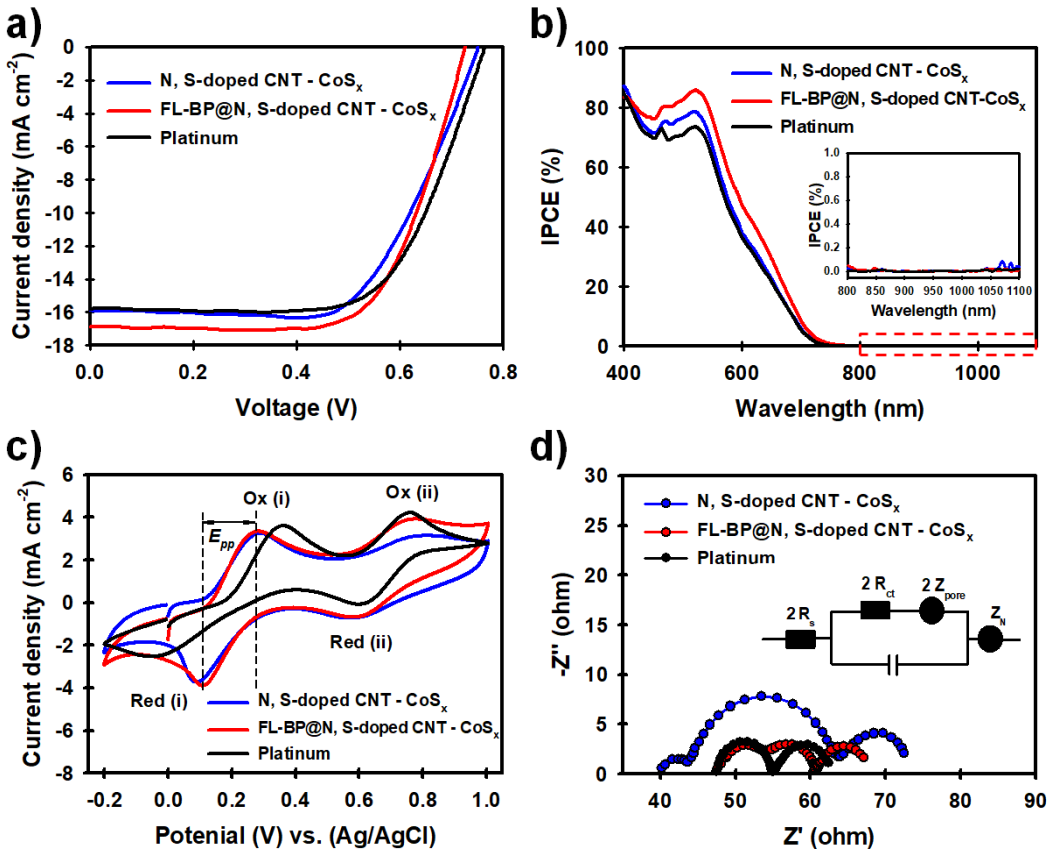

Figure 3. (a) *J-V* curves, (b) IPCE (inset: in the NIR region), (c) CV and (d) EIS spectra of three different electrocatalysts and their corresponding DSSCs.

To attempt to explain our observed improved electrocatalytic activity using FL-BP, we performed density functional-theory (DFT) calculations. To evaluate the electrocatalytic activity of the materials for triiodide reduction (**Figure 4**), calculating the adsorption energy of the I atom on phosphorene is of great importance.[30] The following equation was used to calculate the adsorption energy:

$$E_{ad} = E_{I-P} - \frac{1}{2}E_{I_2} - E_P$$

where, E_{I-P} is the total energy of the phosphorene surface with an adsorbed I atom, E_{I_2} is the total energy of the I_2 molecule, and E_P is the total energy of the pristine phosphorene surface. The calculated E_{ad} of the I atom on phosphorene surface was 0.24 eV, which is small enough to avoid the termination of the reaction that might take place when the I atom binds strongly

to phosphorene. Dissociative adsorption of I_2 on the phosphorene surface provides a ready path to the production of I^- given the relatively low adsorption energy of I on the substrate.

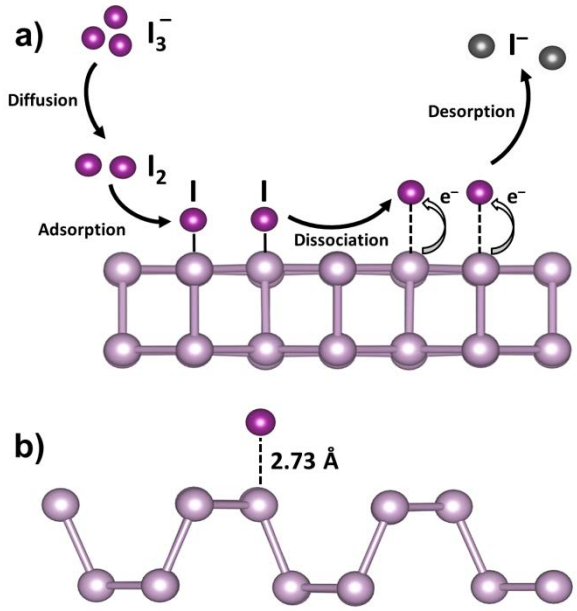

Figure 4. (a) Schematic diagram of the formation, adsorption, dissociation of I_2, and desorption of I^- on phosphorene (armchair). (b) I atom adsorbed on the zigzag directions of phosphorene. The P-I bond distance is 2.73 Å.

In summary, we investigated the electrocatalytic properties of FL-BP sheets produced using a simple and fast MW-assisted LPE method in DSSC systems. To probe the electrocatalytic activity of our FL-BP sheets for the triiodide reduction in DSSCs, we also designed a new class of heteroelectrocatalyst (N, S-doped CNTs–CoS_x). We found based on our experimental results and theoretical calculations the FL-BP sheets show promising electrocatalytic activity toward the reduction of triiodide electrolyte for DSSCs as well as excellent electrochemical stability. The device fabricated with our FL-BP@N, S-doped CNTs–CoS_x heteroelectrocatalyst displayed a PCE of 8.31% which was higher than that of the control Pt based cells. We anticipate that this work will open a window for integrating 2D phosphorene as efficient electrocatalyst materials for various applications.

Acknowledgements

We acknowledge the use of South Australian nodes of the Australian Microscopy & Microanalysis Research Facility (AMMRF) and Australian National Fabrication Facility (ANFF) at Flinders University and the University of Adelaide. The support of the Australian

Research Council Discovery Program (DP150101354 and DP160101301) is gratefully acknowledged.

[1] L. Li, Y. Yu, G. J. Ye, Q. Ge, X. Ou, H. Wu, D. Feng, X. H. Chen, Y. Zhang, *Nat Nanotechnol.* **2014**, *9*, 372.
[2] H. Liu, A. T. Neal, Z. Zhu, Z. Luo, X. Xu, D. Tománek, P. D. Ye, *ACS Nano* **2014**, *8*, 4033.
[3] H. Xiao, Z.-S. Wu, L. Chen, F. Zhou, S. Zheng, W. Ren, H.-M. Cheng, X. Bao, *ACS Nano* **2017**, *11*, 7284.
[4] Y. Zhang, H. Wang, Z. Luo, H. T. Tan, B. Li, S. Sun, Z. Li, Y. Zong, Z. J. Xu, Y. Yang, K. A. Khor, Q. Yan, *Adv. Energy Mater.* **2016**, *6*, 1600453.
[5] X. Zhu, T. Zhang, Z. Sun, H. Chen, J. Guan, X. Chen, H. Ji, P. Du, S. Yang, *Adv. Mater.* **2017**, *29*, 1605776.
[6] C. C. Mayorga-Martinez, Z. Sofer, M. Pumera, *Angew. Chem. Int. Ed.* **2015**, *54*, 14317.
[7] M. Batmunkh, M. Bat-Erdene, J. G. Shapter, *Adv. Energy Mater.* **2017**, DOI: 10.1002/aenm.201701832.
[8] S. Lin, S. Liu, Z. Yang, Y. Li, T. W. Ng, Z. Xu, Q. Bao, J. Hao, C.-S. Lee, C. Surya, F. Yan, S. P. Lau, *Adv. Funct. Mater.* **2016**, *26*, 864.
[9] Y. Yang, J. Gao, Z. Zhang, S. Xiao, H.-H. Xie, Z.-B. Sun, J.-H. Wang, C.-H. Zhou, Y.-W. Wang, X.-Y. Guo, P. K. Chu, X.-F. Yu, *Adv. Mater.* **2016**, *28*, 8937.
[10] S. C. Dhanabalan, J. S. Ponraj, Z. Guo, S. Li, Q. Bao, H. Zhang, *Adv. Sci.* **2017**, *4*, 1600305.
[11] M. Batmunkh, M. Bat-Erdene, J. G. Shapter, *Adv. Mater.* **2016**, *28*, 8586.
[12] V. Eswaraiah, Q. Zeng, Y. Long, Z. Liu, *Small* **2016**, *12*, 3480.
[13] R. Gusmão, Z. Sofer, M. Pumera, *Angew. Chem. Int. Ed.* **2017**, *56*, 8052.
[14] Q. Jiang, L. Xu, N. Chen, H. Zhang, L. Dai, S. Wang, *Angew. Chem. Int. Ed.* **2016**, *55*, 13849.
[15] X. Ren, J. Zhou, X. Qi, Y. Liu, Z. Huang, Z. Li, Y. Ge, S. C. Dhanabalan, J. S. Ponraj, S. Wang, J. Zhong, H. Zhang, *Adv. Energy Mater.* **2017**, *7*, 1700396.
[16] Z.-Z. Luo, Y. Zhang, C. Zhang, H. T. Tan, Z. Li, A. Abutaha, X.-L. Wu, Q. Xiong, K. A. Khor, K. Hippalgaonkar, J. Xu, H. H. Hng, Q. Yan, *Adv. Energy Mater.* **2017**, *7*, 1601285.
[17] R. He, J. Hua, A. Zhang, C. Wang, J. Peng, W. Chen, J. Zeng, *Nano Letters* **2017**, *17*, 4311.
[18] M. Batmunkh, M. J. Biggs, J. G. Shapter, *Small* **2015**, *11*, 2963.
[19] Q. Tang, Y. Duan, B. He, H. Chen, *Angew. Chem. Int. Ed.* **2016**, *55*, 14412.
[20] X. Cui, J. Xiao, Y. Wu, P. Du, R. Si, H. Yang, H. Tian, J. Li, W.-H. Zhang, D. Deng, X. Bao, *Angew. Chem. Int. Ed.* **2016**, *55*, 6708.
[21] I.-Y. Jeon, M. J. Ju, J. Xu, H.-J. Choi, J.-M. Seo, M.-J. Kim, I. T. Choi, H. M. Kim, J. C. Kim, J.-J. Lee, H. K. Liu, H. K. Kim, S. Dou, L. Dai, J.-B. Baek, *Adv. Funct. Mater.* **2015**, *25*, 1170.
[22] M. J. Ju, I.-Y. Jeon, H. M. Kim, J. I. Choi, S.-M. Jung, J.-M. Seo, I. T. Choi, S. H. Kang, H. S. Kim, M. J. Noh, J.-J. Lee, H. Y. Jeong, H. K. Kim, Y.-H. Kim, J.-B. Baek, *Sci. Adv.* **2016**, *2*, e1501459.
[23] M. Bat-Erdene, M. Batmunkh, C. J. Shearer, S. A. Tawfik, M. J. Ford, L. Yu, A. J. Sibley, A. D. Slattery, J. S. Quinton, C. T. Gibson, J. G. Shapter, *Small Methods* **2017**, *1*, 1700260.
[24] M. Bat-Erdene, M. Batmunkh, S. A. Tawfik, M. Fronzi, M. J. Ford, C. J. Shearer, L. Yu, M. Dadkhah, J. R. Gascooke, C. T. Gibson, J. G. Shapter, *Adv. Funct. Mater.* **2017**, DOI: 10.1002/adfm.201704488.
[25] S. Zhang, J. Yang, R. Xu, F. Wang, W. Li, M. Ghufran, Y.-W. Zhang, Z. Yu, G. Zhang, Q. Qin, Y. Lu, *ACS Nano* **2014**, *8*, 9590.
[26] A. Favron, E. Gaufres, F. Fossard, A.-L. Phaneuf-Lheureux, N. Y. W. Tang, P. L. Levesque, A. Loiseau, R. Leonelli, S. Francoeur, R. Martel, *Nat Mater.* **2015**, *14*, 826.
[27] A. Shrestha, M. Batmunkh, C. J. Shearer, Y. Yin, G. G. Andersson, J. G. Shapter, S. Qiao, S. Dai, *Adv. Energy Mater.* **2017**, *7*, 1602276.
[28] K. Qu, Y. Zheng, Y. Jiao, X. Zhang, S. Dai, S.-Z. Qiao, *Adv. Energy Mater.* **2017**, *7*, 1602068.
[29] E. Bi, H. Chen, X. Yang, W. Peng, M. Gratzel, L. Han, *Energy Environ. Sci.* **2014**, *7*, 2637.

[30] Y. Hou, D. Wang, X. H. Yang, W. Q. Fang, B. Zhang, H. F. Wang, G. Z. Lu, P. Hu, H. J. Zhao, H. G. Yang, *Nat. Commun.* **2013**, *4*, 1583.